

pubs.acs.org/acscatalysis Research Article

# Acrolein Hydrogenation Catalyzed by Pt(111): Effect of Carbonaceous Deposits on Kinetics

Mindika Tilan Nayakasinghe, Yang Xu, and Francisco Zaera\*



Cite This: ACS Catal. 2023, 13, 14080-14089



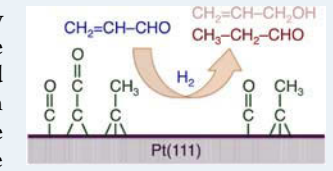
**Read Online** 

**ACCESS** 

Metrics & More

Article Recommendations

ABSTRACT: Absolute turnover frequencies for the hydrogenation of acrolein were measured by using a Pt(111) single crystal as the catalyst. The kinetics of the reaction were found to be somewhat complex because of interference from the simultaneous deposition of strongly adsorbed carbonaceous deposits on the surface, identified here as a mix of ethylidyne, ketene, and carbon monoxide by using in situ reflection—absorption infrared absorption spectroscopy (RAIRS). The fraction of the surface still active for catalysis was titrated as a function of reaction temperature using CO temperature-programmed desorption (TPD), and the resulting values used to estimate



true turnover frequencies, from which an activation energy of  $\sim 15$  kJ/mol was derived. It was found that the buildup of irreversibly adsorbed carbonaceous deposits significantly affects both the activity and the selectivity of the acrolein hydrogenation catalysis, as it does in other olefin hydrogenation processes; propanal is the main product here ( $\sim 90\%$ ), and that requires the preferential hydrogenation of the C=C double bond. On the basis of these results, it is suggested that the catalytic performance of Pt may be improved by modifying the surface to either minimize or change the character of these surface hydrocarbon fragments.

KEYWORDS: hydrogenation selectivity, unsaturated aldehydes, platinum, single crystal, carbonaceous deposits, kinetics, in situ infrared absorption spectroscopy, CO site titration

### 1. INTRODUCTION

Hydrogenation catalysts are used extensively in the chemical industry, and, in spite of much research directed at finding alternatives, most of that catalysis is still promoted with late transition metals. <sup>1–5</sup> Pt in particular promotes many hydrogenations of organic feedstocks with high activity. However, when a reactant exhibits more than one unsaturation, platinum metals tend to lack selectivity. <sup>6</sup> In fact, when different functional groups compete for conversion, the order in which they are hydrogenated with Pt sometimes leads to undesirable products. This is the case in, for instance, the hydrogenation of unsaturated aldehydes, where the most valuable product usually is the unsaturated alcohol, the product of the hydrogenation of the C=O bond, but where Pt mainly promotes the production of the saturated aldehyde via the preferential hydrogenation of the C=C bond instead. <sup>7,8</sup>

Several approaches have been taken to address this problem and improve selectivity in unsaturated aldehyde hydrogenation with Pt-based catalysts. Selection of particular supports, Selection of the size of the metal nanoparticles or the structure of the metal surface, Selection and dopants, and, more recently, the use of additives and dopants, However, it is not always easy to assess the success of the reported approaches, as the activities and selectivities of the catalytic hydrogenations are often reported in a variety of ways, rarely in terms of true turnover frequencies (TOFs) as would be desirable for direct comparisons. It is important to have a benchmark in terms

of the kinetic parameters associated with unsaturated aldehyde hydrogenation promoted by Pt catalysts to compare against.

Here, we provide such a reference for the case of acrolein hydrogenation. Not only do we estimate absolute TOFs in terms of molecules converted per surface Pt atom per unit time, extracted from experiments carried out with a Pt single crystal exposing a (111) plane, but also correct the raw values by the fraction of the metal surface exposed during reaction, given that these reactions are accompanied by the growth of irreversibly bonded carbonaceous deposits, which block catalytic sites. Data are provided as a function of the reaction temperature and partial pressures of the reactants. Both total activity and selectivity toward the three possible products, namely, propanal, allyl alcohol, and propanol, were evaluated and compared against previously reported values to discuss the role that all these parameters and effects play in controlling catalytic performance.

## 2. EXPERIMENTAL DETAILS

The experiments reported here were performed in a two-tier ultrahigh vacuum (UHV) instrument equipped with several

Received: August 16, 2023 Revised: September 29, 2023



techniques and elements for surface cleaning, dosing, and characterization of solid surfaces as well as a so-called highpressure cell (HPC), used for catalytic kinetic studies. As described in previous publications, <sup>33–35</sup> the main level is used for cleaning of the sample, a 1 cm-in-diameter Pt(111) single crystal disk, by a combination of Ar ion bombardment (using an ion gun), annealing, and thermal treatments with O2 (Liquid Carbonic, Research Purity, >99.995%), and for postmortem carbon monoxide temperature-programmed desorption (TPD) surface titration experiments. A UTI 100C quadrupole mass spectrometer was used for the latter, and also to analyze the gas mixtures during the catalytic kinetic studies (see below). This mass spectrometer is interfaced to a personal computer capable of monitoring the evolution of up to 15 chosen masses in the 1-300 amu as a function of both crystal temperature and time.

The second (HPC) level of our surface-science apparatus is accessible with the aid of a horizontal long-travel manipulator also used for surface alignment during the spectroscopic experiments (see below). The Pt(111) crystal was spotwelded to a pair of tantalum wires attached to the copper electrical feedthroughs of the manipulator to allow for liquid-nitrogen cooling and resistive heating in order to set and control its temperature to any value between approximately 100 and 1100 K. The crystal temperature was followed using a chromelalumel thermocouple spotwelded to its side and controlled by a homemade proportional-integral-derivative (PID) circuit. The HPC was designed to perform catalytic kinetic experiments. For that purpose, a small retractable cylindrical cup  $(V_{Cell} \sim 70 \text{ mL})$  mounted on a separate linear translation stage is brought in to fully encase the crystal and isolate it from the UHV environment so that the surface can be exposed to atmospheric pressures of reactive gases. This HPC is incorporated into a 1/4'' stainless-steel-tube loop designed as a gas batch reactor ( $V_{\rm loop} \sim 550$  mL) and equipped with a Baratron capacitance manometer and a stainless-steel bellows circulation pump.

To carry out the catalytic kinetic experiments, the Pt(111)crystal is cleaned in the main chamber, transferred to the second tier, and sealed inside the HPC. Then, the reaction gas mixture is made by combining the desired pressures of the reactants, acrolein (Afla Aesar, 97%; introduced into the loop from the gas manifold via direct evaporation, taking advantage of its high vapor pressure), and H<sub>2</sub> (Airgas, >99.99% purity) in our case, inside the batch reactor's loop and circulating the gases using the bellows pump until they become well mixed, a process that takes approximately 15 min (as determined by following the gas composition versus time, see below). At that point, the HPC, which is bypassed during gas mixing to keep the Pt isolated from the gases, is added to the loop, the system is let to stabilize (a couple of minutes), and the surface is heated to the desired reaction temperature. The composition of the gas mixture is monitored continuously during both the gas mixing and the catalytic reaction stages using the mass spectrometer, by leaking a small amount of the gas into the UHV chamber via a side leak valve. Independent calibration experiments were used to determine that the gas loss from the reactor during reactions due to this leak is negligible, less that 2% of the total pressure after a 2.5 h reaction run, and that the delay in gas sampling due to diffusion from the reaction loop to the UHV chamber through the tubing and leak valve is also minimal, less than 10 s.

The raw mass-spectrometer data from the kinetic experiments were analyzed quantitatively via their deconvolution using measured mass spectrometry cracking patterns for all the reactants and products (using our setup) and a procedure described elsewhere. 33,36 Typically, the signals for 56, 57, 58, and 31 amu were selected for these calculations, to represent the partial pressures of acrolein (2-propenal), allyl alcohol (2propenol), propanal, and 1-propanol, respectively, the latter three being the main products expected from acrolein hydrogenation. The kinetic data were converted into turnover numbers (TONs, in units of number of molecules per Pt surface atom) using an independent mass-spectrometer signal calibration relating voltages to gas pressures, the volume of the reactor, and the surface area of the Pt surface (based on a value of  $1.5 \times 10^{15}$  atoms/cm<sup>2</sup> for the surface atom density in Pt(111)). To facilitate the data analysis, the raw kinetic data, expressed as number of molecules per Pt atom  $(N_{
m Molecules}/N_{
m Pt})$ a number directly related to TON) versus reaction time, were empirically fitted to exponential functions; turnover frequencies (TOFs) were then calculated by numerical derivatization of the TON-versus-time plots and reported in units of TOF = TON/s.

For the CO TPD titration experiments, the HPC was evacuated and retracted after the kinetic runs, which typically lasted 75 min, and the Pt(111) crystal was transferred back to the main chamber. It was then cooled below 150 K and dosed with 3 L of CO (1 L = 1 × 10<sup>-6</sup> Torr s; CO, 99.5% purity, Matheson Tri-Gas), after which the surface temperature was ramped at a constant heating rate of 10 K/s while recording the mass spectrometer signal for 28 amu. The TPD signal intensities are reported in arbitrary units, but surface coverages ( $\theta$ ) were estimated by integration of the areas of the CO TPD peaks relative to that obtained for a clean Pt(111) surface ( $\theta_{\text{clean}}$ ), which is assigned a value of unity.

Two small NaCl windows were added at opposite sides of the lateral walls of the main body of the HPC to allow for the performance of in situ or operando spectroscopic characterization of the surface with reflection-absorption infrared spectroscopy (RAIRS) during the course of the catalytic reactions. The IR beam from a Bruker Equinox 55 Fouriertransform infrared (FT-IR) spectrometer is passed through a polarizer and made to travel in and out of the reactor volume through the NaCl windows, focusing it onto the sample at a grazing incidence (~85°) by using long focal length (12 in.) parabolic mirrors, before collecting it onto a narrow-band mercury-cadmium-telluride (MCT) detector. The entire beam path is enclosed in a sealed box purged with dry air and purified by using a scrubber (Balston 75-60) for the removal of CO<sub>2</sub> and water. All spectra were acquired by averaging the data from 2000 scans taken at a resolution of 4 cm<sup>-1</sup>, a process that takes about 4 min per experiment, and ratioed against spectra from the clean sample obtained in the same way but before gas dosing. Spectra were taken with both s- and p-polarized light to discriminate between gas-phase and adsorbed species.<sup>37</sup>

### 3. RESULTS

Kinetic data for the hydrogenation of acrolein with  $\rm H_2$  promoted by a Pt(111) single-crystal surface were acquired by following the evolution of the partial pressures of the main reactants and products over time at a constant temperature using mass spectrometry. The data recorded during a typical run are shown in the left panel of Figure 1, in that case for the

ACS Catalysis pubs.acs.org/acscatalysis Research Article

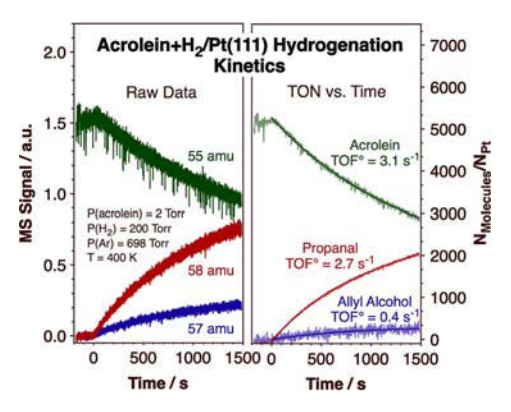


**Figure 1.** Typical results from a catalytic run for the conversion of acrolein in a  $\rm H_2$  atmosphere promoted by a Pt(111) surface. Left: raw mass spectrometer signals for 55, 57, and 58 amu as a function of reaction time, for the conversion of a reaction mixture consisting of 2 Torr of acrolein, 200 Torr of  $\rm H_2$ , and 698 Torr of Ar, at 400 K. Right: same data after analysis of the raw signals to obtain TON equivalents ( $N_{\rm Molecules}/N_{\rm Pt}$ ) for acrolein, propanal, and allyl alcohol. The start of the reaction, time = 0, was set at the point when the surface reached the desired temperature (400 K in this case). The smooth solid lines drawn through the raw data correspond to exponential fits.

conversion of a mixture of 2 Torr of acrolein, 200 Torr of H<sub>2</sub>, and 698 Torr of Ar (used as a ballast gas to facilitate gas recirculation in our batch reactor) at a crystal temperature of 400 K. Several masses were followed simultaneously to represent the key compounds involved in this reaction, from which the signals for 55, 57, and 58 amu are shown here. The raw data were deconvoluted using a procedure mentioned in Experimental Section and published in more detail elsewhere, 33,36 and the signals calibrated to convert them into partial pressures and from there into turnover number (TON) equivalents (number of molecules per Pt atom, or  $N_{\text{Molecules}}$  $N_{\rm Pt}$ ); the results of this analysis are presented in the right panel of Figure 1. As expected, the signal for acrolein is seen to decrease and those of the products to grow with increasing reaction time. The main product under these reaction conditions was propanal, but a small amount of allyl alcohol was detected as well, approximately 10-15% of the total acrolein consumed; no significant propanol was seen in any of our kinetic runs. A mass balance was retained in all cases within a margin of 5% of the total pressure throughout the course of the reaction, a test of the viability of our data analysis.

In order to minimize interference from the noise of the kinetic data, the processed values in the right panel of Figure 1 were fitted to exponential curves (shown as solid lines in the figure). This choice was made empirically but is justified by the near-unity reaction order of the acrolein conversion rate on acrolein partial pressure determined from the experiments reported below. Initial turnover frequencies (TOF°) were then estimated from the slope of the tangent of those lines at t = 0. As indicated in Figure 1,  $TOF^{\circ}$  values of 3.1, 2.7, and 0.4 s<sup>-1</sup> were determined in this example for the acrolein consumption and for the propanal and allyl alcohol production, respectively. It is interesting to note that, in an early study on the hydrogenation of crotonaldehyde on Pt(111) (the only other study that we are aware of where the kinetics of this type of reaction has been measured on Pt(111) single crystals), much lower TOF values were reported, 2 orders of magnitude below ours.<sup>40</sup> We can only speculate on why that may be. In that study, the reaction temperatures used were in general lower

than ours, but the estimated activation energies were also an order of magnitude higher than what we report here (see below). As in our case, their catalyst was irreversibly poisoned over time with carbonaceous deposits, but their measured carbon coverages, using Auger electron spectroscopy, are quite large, even though their reaction was carried out at low temperatures; perhaps it is this excessive poisoning (possibly due to experimental artifacts) that rendered their surfaces so inactive. We do believe that our estimates of the TOF°s for acrolein hydrogenation with Pt(111) are more realistic, in line with what is known from other hydrogenation reactions. 35,41,42

The evolution of the TOF values could also be followed as a function of reaction time, via numerical derivation of the raw data in Figure 1-right, or, to minimize the noise level, via analytical derivation of the fitted exponential curves; the results from the second approach are reported in the left panel of Figure 2. As expected, the rates of conversion of acrolein as

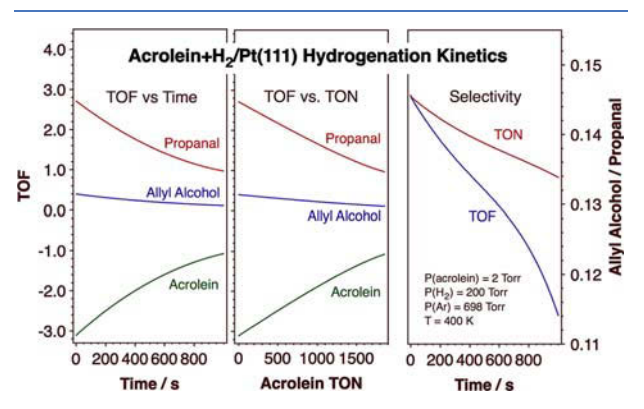


Figure 2. Processed kinetic data from the results reported in Figure 1. Left: TOFs versus time for acrolein, propanal, and allyl alcohol, obtained by analytical derivation of the exponential curves fitted to the TON versus time data in the right panel of Figure 1. Center: same data plotted in the form of TOFs versus acrolein TON. Right: selectivity, expressed as the TON and TOF ratios of allyl alcohol versus propanal production.

well as those of the production of propanal and allyl alcohol all decrease in magnitude with time, as the reactant is consumed. The same data are plotted in the form of TOF vs acrolein TON in the center panel of Figure 2 to better highlight this correlation. The close-to-linear dependence of those two parameters attests to the approximately first order dependence of the reaction rates on the acrolein partial pressure, the assumption that was made to fit the TON-versus-time data to exponential curves. It should be pointed out that all reactions in this study were carried out using a large excess of H<sub>2</sub>, so the contribution of that pressure to the reaction rates can be considered constant. In terms of selectivity, its time dependence can be extracted from the data in the right panel of Figure 2, where both the TON and TOF allyl alcohol-to-propanal ratios are plotted versus time. The selectivity toward allyl alcohol production appears to decrease with reaction time, possibly as irreversibly adsorbed carbonaceous deposits build up on the surface (more on this later), but the effect is subtle, on the order of 10%, and not entirely reliable since in many cases the allyl alcohol production is too low to be detectable.

A more complete study of the dependence of the reaction rates on the partial pressures of the reactants was performed by measuring the initial  $TOF^{\circ}s$  of the reaction as a function of the initial acrolein and  $H_2$  partial pressures, which were varied

independently, one at a time, while keeping the other constant. The results are presented in Figure 3 in the form of the

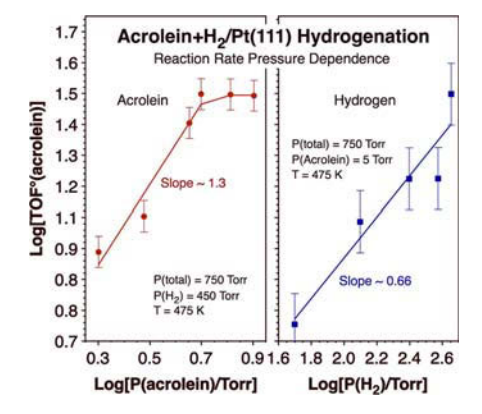


Figure 3. Dependence of the initial acrolein conversion rates ( $TOF^{\circ}s$ ) at 450 K on the partial pressures of acrolein (left panel) and  $H_2$  (right). The data are plotted in log-log form in order to extract reaction rate orders from the slopes. Nonlinear behavior is observed with acrolein.

logarithm of the TOF°s for acrolein versus the logarithm of the partial pressures of either reactant. As seen in the right panel of that figure, the order with respect to H2 was estimated to be approximately 2/3, somewhere between 0.5, which would indicate a rate-limiting step involving atomic surface hydrogen (H<sub>ads</sub>), and 1, in which case the limiting step would involve molecular hydrogen. This intermediate value may reflect a number of factors, including a competition with acrolein for adsorption sites and a Langmuir-type isothermal uptake of hydrogen on the surface, which would show a linear dependence of the hydrogen surface uptake on  $P(H_2)$  at low pressures but a leveling off at higher pressures. Regardless, a variable reaction order on H2 between 0.5 and 1 is common in hydrogenation reactions.<sup>2,43</sup> The behavior of the reaction rates with respect to the acrolein partial pressure is also complex, starting with a value larger than  $1 (\sim 1.3)$  at low pressures but approaching zero at higher pressures (Figure 3-left). The transition is relatively sharp and therefore not fully accounted for by Langmuir-type kinetics; therefore, additional factors may be at play. Our explanation for the behavior seen in both cases relates to the concurrent partial poisoning of the surface by the formation of carbonaceous deposits, as discussed in more detail below.

Data on the temperature dependence of the initial reaction rates for acrolein hydrogenation on the Pt(111) surface are provided in the left panel of Figure 4 (open red squares and dashed line). Again, a complex behavior was observed, with significant deviations from Arrhenius behavior: the TOF $^{\circ}$  value increases with increasing reaction temperature in the range from 357 to 543 K, as expected for an activated process, but then decreases at higher temperatures.

One clue for the reason that the rate dependence on acrolein partial pressures and temperature is complex comes from experiments designed to test the stability of the catalyst. The left panel of Figure 5 shows the results from an experiment where 5 consecutive runs were carried out on the same catalyst without cleaning of the surface in between: only the old reaction mixture was pumped out and a new identical fresh one was added to the reactor volume in between runs. It can be seen there that the activity of the catalyst is initially fast but

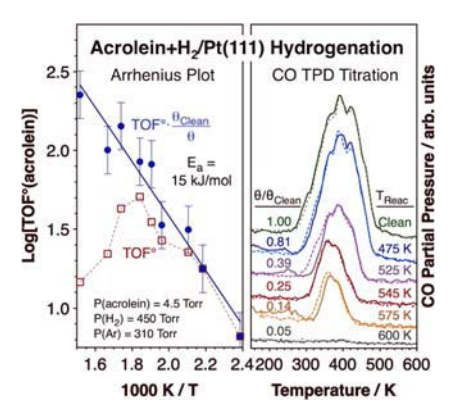
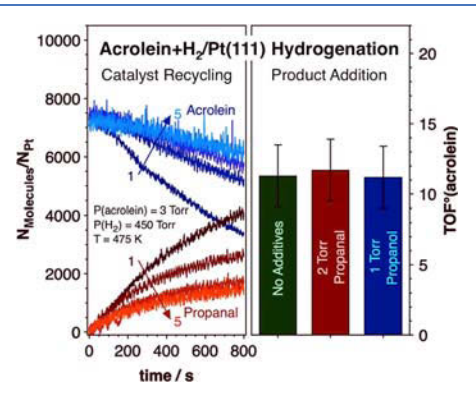


Figure 4. Left: Arrhenius plot of TOF° vs reaction temperature. The raw data are displayed as open red squares and a dashed line, whereas the values corrected by the fraction of the surface available for reaction are shown as filled blue circles. A linear fit to the latter set, shown as a blue solid line, yielded a value for the activation barrier of 15 kJ/mol. Right: CO TPD titration traces obtained after 75 min of reaction as a function of reaction temperature. Reaction conditions:  $P(\text{acrolein}) = 4.5 \text{ Torr}, P(\text{H}_2) = 450 \text{ Torr}, P(\text{Ar}) = 310 \text{ Torr}.$  For the TPD experiments, the surface was saturated with 3 L of CO at 150 K before ramping the temperature ramping 10 K/s. Two traces are shown for each temperature, with solid and dashed lines, from two independent experiments to highlight the reproducibility of the data.



**Figure 5.** Reaction kinetics for the conversion of gas mixtures made out of 3 Torr of acrolein plus 450 Torr of  $H_2$  promoted at 475 K by a Pt(111) surface. Left: Consumption of acrolein and production of propanal as a function of time from five consecutive runs using fresh reaction mixtures but the same untreated catalyst to highlight the gradual poisoning of the surface of the catalyst via the deposition of irreversibly adsorbed carbonaceous deposits. Right: TOF°s from conversion of acrolein +  $H_2$  reaction mixtures, alone and with either 2 Torr of propanal or 1 Torr of propanol added. Similar values were measured in all three experiments, ruling out the buildup of products in the reaction mixture over time as the reason for the poisoning of the catalytic activity.

reaches a much lower value asymptotically as subsequent catalytic runs are carried out. In fact, a slowing down of the reaction is even evidenced in the first run by the bending of the curves for both acrolein consumption and propanal production with time. This behavior is not surprising, and it has been ascribed in other systems to the blocking of surface sites by the formation of irreversibly adsorbed carbon-containing organic residues. <sup>35,44–46</sup> As we discuss below, such an explanation fits our experimental results as well.

An alternative explanation for the slow poisoning of the catalytic activity in this system over time could be that the

products generated by the hydrogenation reaction may compete for adsorption sites with the reactant, thus blocking some and slowing down the conversion. This hypothesis was tested here by performing kinetic experiments with reaction mixtures containing such possible poisoning byproducts. The right panel of Figure 5 contrasts the TOF° obtained for the conversion of 3 Torr of acrolein and 450 Torr of  $\rm H_2$  at 475 K with results from runs where either 2 Torr of propanal or 1 Torr of propanol were added to the reaction mixture. The same TOF° was measured in all three cases within the accuracy of our experiments; no poisoning effect was observed due to the buildup of products in our batch reactor during the course of the reaction.

The irreversible deposition of organic residues on the surface during reaction, a phenomenon that is well established and that is seen in most hydrocarbon hydrogenation processes, 35,44-46 is therefore the most viable explanation for the kinetics reported above. To quantify the extent of this effect, the Pt sites exposed for catalytic activity were titrated after ~75 min of reaction by transferring the surface to the main UHV environment, saturating it with CO, and performing a TPD experiment. The CO desorption data obtained this way are shown as a function of the reaction temperature in the right panel of Figure 4. The traces obtained for the clean surface (top, green lines) show a broad feature between 300 and 500 K, consistent with what has been previously reported in the literature. 47,48 Two trends are observed in the CO titration results in Figure 4-right as a function of increasing reaction temperature: (1) the total area of the CO TPD peak decreases, an indication of the reduction in the number of Pt sites available for reaction, and (2) the remaining CO TPD peak signal appears on the low-temperature side of the traces, indicating that the surface poisoning occurs selectively at the sites that bind CO the most strongly. Strong CO binding is typically associated with low coordination sites such as steps, kinks, and other defects, <sup>49,50</sup> and results from previous CO titration experiments using FTIR have indicated that our Pt(111) single-crystal surface has approximately 5–10% defect sites,<sup>51</sup> which may be the first to decompose incoming reactant molecules and form irreversibly adsorbed species.<sup>52</sup> In addition, it has also been previously determined that the deposition of carbonaceous deposits on the Pt(111) surface leads to a weakening of the CO bond to the surface, 53 another possible explanation for the shift of the CO TPD signal toward lower temperatures in Figure 4-right.

This reduction in the surface area for catalysis due to the deposition of carbonaceous deposits clearly affects the activity of the catalyst. In order to estimate the intrinsic catalytic activity of the Pt surface atoms for the promotion of acrolein hydrogenation, the TOF° values reported as open red squares in the left panel of Figure 4 were scaled accordingly: the new results are shown in the same figure as solid blue circles. With this correction, the temperature dependence of the rates better follows the expected Arrhenius behavior. A linear fit to the new data (blue solid line in the left panel of Figure 4) provides an estimate for the activation barrier of 15 kJ/mol. This is a low value, but not out of line with what is expected for hydrogenation catalysis with Pt, including in cases with unsaturated aldehydes. 7,55,56 The degree of surface poisoning also changes with the composition of the reaction mixture, but in a less dramatic way. The fraction of uncovered Pt after reaction is plotted as a function of the molar fraction of acrolein in the acrolein + H2 mixture in Figure 6. Counter-

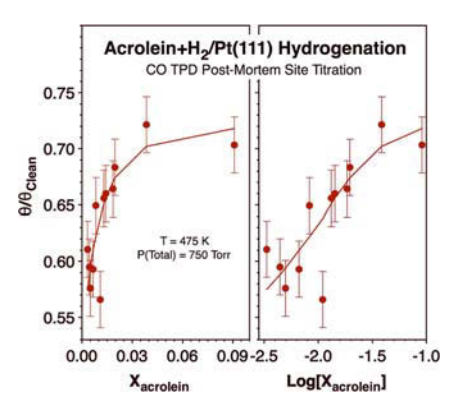


**Figure 6.** Fraction of Pt surface atoms that remains uncovered after 75 min of reaction  $(\theta/\theta_{\text{Clean}})$  as a function of the molar fraction of acrolein  $(X_{\text{acrolein}})$  in the initial reaction mixture. Both linear (a) and logarithmic (b) scales are used for  $X_{\text{acrolein}}$ , the latter provided to better display the data in the low coverage (<0.02) range. Reaction conditions: P(total) = 750 Torr, T = 475 K.

intuitively, more Pt surface sites remain available for catalysis the richer the reaction mixture is in the unsaturated aldehyde, but in all cases that fraction remains in a range between approximately 60 and 70% of the total Pt surface atoms in the Pt(111) crystal (at 475 K).

Finally, in situ reflection—absorption infrared absorption spectroscopy (RAIRS) experiments were performed to identify the nature of the irreversibly adsorbed organic fragments that block the Pt surface sites. Figure 7 reports the resulting data for

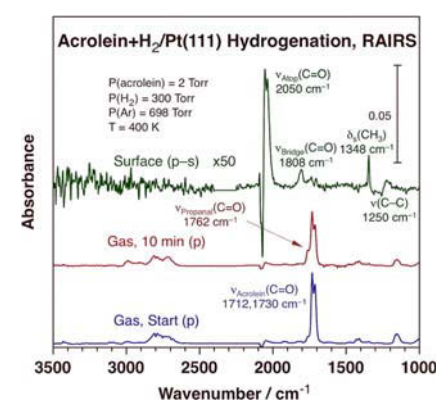


**Figure 7.** RAIRS data obtained in situ during an acrolein hydrogenation catalytic run. The two bottom traces correspond to the results recorded with p-polarized light at the start of the reaction (bottom, blue) and after 10 min (middle, red), whereas the top trace (green) was obtained via subtraction of the data obtained with s-polarized light from that acquired with p-polarized light to isolate the spectrum originated from IR absorption by the adsorbed species. Reaction conditions: P(acrolein) = 2 Torr,  $P(\text{H}_2) = 300 \text{ Torr}$ , P(Ar) = 698 Torr, and T = 400 K.

a typical example. Unprocessed, the spectra are dominated by the gas-phase species, a fact that affords corroboration of the progress of the acrolein hydrogenation reaction. Indeed, in the RAIRS spectrum obtained at the start of the reaction (bottom, blue trace), only peaks associated with gas-phase acrolein are detected, including those around 1150 cm<sup>-1</sup> due to a C–C stretching motion ( $\nu$ (C–C)), 1410 and 1430 cm<sup>-1</sup> from CH<sub>2</sub> deformations ( $\delta$ (CH<sub>2</sub>)), and 1712 and 1730 cm<sup>-1</sup> from C=O stretching modes ( $\nu$ (C=O)), and also several peaks in the

2700–3000 cm<sup>-1</sup> region associated with C–H stretching modes ( $\nu$ (C–H)). After 10 min of reaction, on the other hand, new features start to develop at 1385 (methyl symmetric deformation, or umbrella, mode,  $\delta_{\rm s}({\rm CH_3})$ ), 1762 ( $\nu$ (C=O)), and 2720 and 2990 ( $\nu$ (C–H)) cm<sup>-1</sup>, all assignable to gasphase propanal, the main product of acrolein hydrogenation (Figure 7, middle, red trace).

No spectroscopic peaks corresponding to surface species are discernible in the two spectra discussed above, but, by subtracting from the p-polarized spectrum similar data obtained with s-polarized light, the surface features can be extracted, taking advantage of a well-known surface selection rule applicable to RAIRS with metals.<sup>38,57</sup> The new trace (Figure 7, top, green), amplified by a factor of 50, clearly shows new peaks at 1250, 1348, 1705, 1737, 1808, and 2050 cm<sup>-1</sup>. The assignment of those peaks to surface species is facilitated by our previous characterization of the thermal chemistry of acrolein on Pt(111) since, as it turns out, the spectrum reported here matches quite well that obtained after annealing the adsorbed aldehyde under vacuum to temperatures between 280 and 340 K. 58,59 In the previous study, we concluded that the peaks at 1250 ( $\nu$ (C-C)) and 1348 ( $\delta_s$ (CH<sub>3</sub>)) cm<sup>-1</sup> identify ethylidyne (Pt<sub>3</sub>=C-CH<sub>3</sub>),60,61 a well-known surface species seen during many other catalytic olefin hydrogenation reactions.<sup>35,62-70</sup> The peaks at 1705 and 1737 cm<sup>-1</sup>, on the other hand, are characteristic of carbonyl stretching modes in organic molecules ( $\nu(C=O)$ ), although the latter could also be associated with C=C motions ( $\nu$ (C=C)); they may originate from ketene or similar surface species. Finally, the last two peaks, at 1808 and 2050 cm<sup>-1</sup>, are assigned to CO bonded to bridge and atop Pt sites, respectively. 51,71,72 CO, and possibly ketene, may be displaced from the surface by the gas molecules in the reaction mixture,<sup>73</sup> but ethylidyne is much more difficult to remove and is likely to be the main surface species blocking catalytic sites as the hydrogenation catalysis progresses.

# 4. DISCUSSION

As stated in the introduction, one of the objectives of this work was to obtain reference kinetic data for the catalytic hydrogenation of acrolein promoted by metallic Pt. A Pt(111) single crystal was used both to eliminate any contribution from other surfaces, in particular any support, and to deal with a well-defined surface, in this case, the hexagonal closed-packed (111) plane of the fcc structure of Pt crystals. Having such control of the nature of the catalytic surfaces, absolute values for turnover frequencies (TOFs) were measured as a function of temperature and acrolein and hydrogen partial pressures. It was found that, in spite of taking the precautions mentioned above, the kinetics of the hydrogenation reaction are complex and not easily described by a simple power rate law. Specifically, the rate dependence on acrolein partial pressure is approximately first order at low pressures but levels off and transitions to zero order at higher pressures. This trend may be explained in part by a Langmuirtype adsorption behavior in which the pressure dependence diminishes as the surface becomes saturated with the adsorbate, but the sharpness of the transition seen here cannot be fully accounted for by such model. Moreover, the value of the reaction rate order with respect to the pressure of hydrogen is somewhere between 1/2 and 1, suggesting a competition between two rate limiting steps involving atomic and molecular hydrogen, respectively: the uptake of H<sub>2</sub> on the (partially

covered) Pt(111) surface may display rates comparable to those of the next step, the incorporation of the first hydrogen atom into an unsaturated bond in acrolein (most likely the C=C bond). The absolute TOF values were found to be in the range between approximately 3 and 50 (molecules of acrolein converted per Pt surface atom per second), with the main product being propanal (from hydrogenation of the C=C bond). These numbers are high relative to those of most other catalytic reactions, but similar to what has been reported for the hydrogenation of olefins, and the pressure dependence is equally consistent with previous reports, 2,74 including with work carried out using Pt nanoparticles or Pt single crystals. 41,42,76

The changes in TOF°s with surface temperature are also not straightforward to explain, as they do not follow an Arrhenius behavior: the rates do increase with increasing temperature at first but reach a maximum at approximately 540 K and then go down. It was also determined that such rates decrease with time of reaction and do not return to their initial value even if a fresh reaction mixture is added to the reactor. As for the reason for this, it was determined that the poisoning is not due to interference from the products. This is a factor that needed to be considered here because ours is a batch reactor where the products accumulate in the reaction mixture over time; that was ruled out on the basis of the measurement of similar rates with reaction mixtures initially spiked with either propanal or propanol. Instead, all the experimental results indicate that the Pt surface becomes poisoned by the buildup of irreversibly adsorbed carbonaceous deposits. This is not surprising, as such behavior has already been widely reported for the hydrogenation of olefins. 35,77,78 Here, the fraction of the Pt surface uncovered and available for catalytic promotion was estimated post mortem via titration with CO and quantification of the resulting TPD data. As expected, more of the surface becomes covered with carbonaceous deposits at higher reaction temperatures, a trend that justifies the decrease in apparent hydrogenation rates above 540 K. After correcting for this factor, an Arrhenius behavior was seen, and an activation barrier of 15 kJ/mol was estimated from the kinetic data. Again, that is a value consistent with what is expected for C= C bond hydrogenation catalysis. 2,41,42,74-76

As per the nature of the carbonaceous deposits that build up on the Pt surface during reaction, in situ infrared spectroscopy data indicated that those are composed mainly of ethylidyne, ketene, and carbon monoxide. The latter two have already been reported as decomposition products from the thermal activation of acrolein on Pt(111) under UHV. S8,59 Regarding ethylidyne, this is a very common surface species produced by the dehydrogenation of ethylene (another decomposition product from acrolein) on metals.  $^{35,41,67,68,79-81}$  It is possible to displace CO from metal surfaces under atmospheric pressures of other gases,  $^{73}$  but ethylidyne is more difficult to remove and likely to persist as long as there is acrolein (or another unsaturated hydrocarbon) present in the gas mixture.  $^{35,65}$ 

All aspects of the kinetics of hydrogenation of acrolein on Pt(111) discussed above parallel those seen with olefins as reactants. In fact, it is the hydrogenation of acrolein to propanal that dominates this process, also an olefin hydrogenation reaction; the production of allyl alcohol or propanol is minimal under the reaction conditions reported here. This undesirable selectivity to the production of the saturated aldehyde is what has been reported with supported Pt

catalysts,<sup>7,8</sup> and also what can be expected given the propensity of unsaturated aldehydes to adsorb on Pt surfaces via their C= C bond. 82-87 On the other hand, it is somewhat different to what we have reported previously on the basis of studies under UHV using high-flux molecular beams, 88 which showed that full hydrogenation to the saturated alcohol can be a primary product, accounting for as much as 40% of the total hydrogenated compounds. The explanation for this difference relates again to the concomitant deposition of carbonaceous deposits on the surface during reaction. In our extensive past studies on olefin hydrogenation promoted by Pt surfaces, we have learned that the coverages of these deposits depend on both the gas mixture composition, that is, the ratio of the hydrocarbon to H2, and the total pressure, and that such variations in coverage significantly affect the kinetics of the C=C hydrogenation reactions. 89 With hydrogen-rich mixtures, the surface remains relatively clean, the hydrogenation rate is approximately first order in P(H2), and the hydrogenation probability is close to unity. As the relative partial pressure of the organic reactant is increased, however, the surface becomes more crowded with irreversible adsorbates, the rate order on hydrogen slowly approaches zero, and the reaction probability becomes smaller. We estimate that while in our previous molecular beam experiments we were probing the former pressure regime, here we are closer to the latter; this is also the regime applicable to most realistic catalytic processes.

The implications of our results are straightforward: the irreversible deposition of carbonaceous deposits such as ethylidyne that accompany the catalytic hydrogenation of unsaturated aldehydes affects both the activity and the selectivity of the reaction. Because this is a natural process that accompanies most hydrocarbon hydrogenations, it could be thought that there is not much that can be done about it. However, this knowledge can guide our thinking when designing new catalysts. For one, the alloying of Pt with a second metal such as Sn can reduce carbonaceous growth; this is a well-established strategy in oil refining processes, 90,91 and has also been tested with unsaturated aldehydes, although the rationale offered in that work has been that modification of the electronic properties of Pt may favor specific aldehyde hydrogenation steps (not that it reduces the amount of carbon deposition on the surface, which it does). 28,92-94 More recently, it has been suggested that selectivity in many catalytic reactions may be tuned via surface modification with specific organic modifiers. 46,95 In our context, this is a way to exert some control over the coverage and nature of the carbonaceous deposits rather than letting those develop organically during the catalysis. 6 These and other strategies can be developed to reduce or direct the formation of strongly adsorbed species on the surface and with that tune reaction selectivity in hydrogenation catalysis.

## 5. CONCLUSIONS

The kinetics of the hydrogenation of acrolein promoted by Pt(111) surfaces was measured as a function of both the temperature and the partial pressures of the reactants. The main product detected was propanal, but about 10-15% of the initial acrolein is converted to allyl alcohol. The reaction rate order with respect to hydrogen was determined to be approximately 0.66 within the range of conditions used in our experiments, suggesting that the steps associated with  $H_2$  adsorption and the first H addition to acrolein may exhibit

comparable rates. The reaction rate order with respect to acrolein was estimated to be above 1 at low pressure but to approach zero at higher pressures, a behavior possibly reflecting Langmuir-type kinetics for the acrolein uptake and also surface poisoning. Indeed, experiments where the catalyst was recycled without any treatment in between indicated that the reaction rates decrease steadily over time until reaching a steady-state value, and additional tests where either propanal or propanol was added to the initial reaction mixture proved that such poisoning is not due to the accumulation of products in the gas phase. Instead, it was determined that the reason for the variable kinetics with time is the buildup of irreversibly adsorbed carbonaceous fragments on the surface. The extent of this deposition increases with reaction temperature, and, as a consequence, an optimal catalytic performance was seen at 540 K; beyond that point, the overall reaction rate decreases with increasing temperature. The fraction of the surface sites blocked by these deposits was estimated by performing post mortem CO TPD titrations, and the apparent turnover frequencies estimated from our catalytic runs normalized by that factor to obtain absolute values of the number of acrolein molecules converted per exposed Pt surface atom per unit time. An Arrhenius plot of those corrected data followed a linear trend, from which a value of approximately 15 kJ/mol was estimated for the activation energy of the reaction. In terms of the nature of the carbonaceous deposits that poison the surface during catalysis, in situ infrared absorption spectroscopy data indicated the formation of ethylidyne, ketene, and CO, the same products seen during the thermal decomposition of acrolein adsorbed on Pt(111) under vacuum. In summary, it was concluded that the growth of the carbonaceous layer on the Pt surface that accompanies most hydrocarbon conversion catalysis affects both the activity and the selectivity of the hydrogenation of acrolein.

## AUTHOR INFORMATION

# **Corresponding Author**

Francisco Zaera — Department of Chemistry, University of California, Riverside and UCR Center for Catalysis, Riverside, California 92521, United States; orcid.org/0000-0002-0128-7221; Email: zaera@ucr.edu

#### Authors

Mindika Tilan Nayakasinghe — Department of Chemistry, University of California, Riverside and UCR Center for Catalysis, Riverside, California 92521, United States; Present Address: Intel Corporation, Hillsboro, OR 97124, USA

Yang Xu — Department of Chemistry, University of California, Riverside and UCR Center for Catalysis, Riverside, California 92521, United States

Complete contact information is available at: https://pubs.acs.org/10.1021/acscatal.3c03870

#### Notes

The authors declare no competing financial interest.

### ACKNOWLEDGMENTS

Financial support for this research was provided by the U.S. National Science Foundation, Division of Chemistry, under contract no. NSF-CHE2244925.

**ACS Catalysis** pubs.acs.org/acscatalysis Research Article

## REFERENCES

- (1) Rylander, P. Catalytic Hydrogenation over Platinum Metals; Academic Press: New York, 1967.
- (2) Bond, G. C. Metal-Catalysed Reactions of Hydrocarbons; Springer: New York, 2005; p 666.
- (3) Mäki-Arvela, P.; Holmbom, B.; Salmi, T.; Murzin, D. Y. Recent Progress in Synthesis of Fine and Specialty Chemicals from Wood and Other Biomass by Heterogeneous Catalytic Processes. Catal. Rev. 2007, 49, 197-340.
- (4) Ma, Z.; Zaera, F. Heterogeneous Catalysis by Metals. In Encyclopedia of Inorganic and Bioinorganic Chemistry; Scott, R. A., Ed.; John Wiley & Sons, Ltd: Chichester, 2014; p eibc0079.
- (5) Besson, M.; Gallezot, P.; Pinel, C. Conversion of Biomass into Chemicals over Metal Catalysts. Chem. Rev. 2014, 114, 1827-1870.
- (6) Augustine, R. L. Selective Heterogeneously Catalyzed Hydrogenations. Catal. Today 1997, 37, 419-440.
- (7) Gallezot, P.; Richard, D. Selective Hydrogenation of  $\alpha,\beta$ -Unsaturated Aldehydes. Catal. Sci. Technol. 1998, 40, 81-126.
- (8) Wang, X.; Liang, X.; Geng, P.; Li, Q. Recent Advances in Selective Hydrogenation of Cinnamaldehyde over Supported Metal-Based Catalysts. ACS Catal. 2020, 10, 2395-2412.
- (9) Claus, P. Selective Hydrogenation of  $\alpha,\beta$ -Unsaturated Aldehydes and Other C = O and C = C Bonds Containing Compounds. Top. Catal. 1998, 5, 51-62.
- (10) Mäki-Arvela, P.; Hájek, J.; Salmi, T.; Murzin, D. Y. Chemoselective Hydrogenation of Carbonyl Compounds over Heterogeneous Catalysts. Appl. Catal., A 2005, 292, 1-49.
- (11) Lan, X.; Wang, T. Highly Selective Catalysts for the Hydrogenation of Unsaturated Aldehydes: A Review. ACS Catal. 2020, 10, 2764-2790.
- (12) Ammari, F.; Lamotte, J.; Touroude, R. An Emergent Catalytic Material: Pt/ZnO Catalyst for Selective Hydrogenation of Crotonaldehyde. J. Catal. 2004, 221, 32-42.
- (13) Chiu, T.-C.; Lee, H.-Y.; Li, P.-H.; Chao, J.-H.; Lin, C.-H. Effects of Interfacial Charge and the Particle Size of Titanate Nanotube-Supported Pt Nanoparticles on the Hydrogenation of Cinnamaldehyde. Nanotechnology 2013, 24, 115601.
- (14) Ji, X.; Niu, X.; Li, B.; Han, Q.; Yuan, F.; Zaera, F.; Zhu, Y.; Fu, H. Selective Hydrogenation of Cinnamaldehyde to Cinnamal Alcohol over Platinum/Graphene Catalysts. ChemCatChem 2014, 6, 3246-
- (15) Liu, H.; Li, Z.; Li, Y. Chemoselective Hydrogenation of Cinnamaldehyde over a Pt-Lewis Acid Collaborative Catalyst under Ambient Conditions. Ind. Eng. Chem. Res. 2015, 54, 1487-1497.
- (16) Gao, Z.; Cai, L.; Miao, C.; Hui, T.; Wang, Q.; Li, D.; Feng, J. Electronic Metal-Support Interaction Strengthened Pt/Coal-Ldhs Catalyst for Selective Cinnamaldehyde Hydrogenation. ChemCatChem 2022, 14, No. e202200634.
- (17) Liang, Y.; Tang, Q.; Liu, L.; Wang, D.; Dong, J. Fabrication of Highly Oxidized Pt Single-Atom Catalysts to Suppress the Deep Hydrogenation of Unsaturated Aldehydes. Appl. Catal., B 2023, 333,
- (18) Serrano-Ruiz, J. C.; Lopezcudero, A.; Sollagullon, J.; Sepulvedaescribano, A.; Aldaz, A.; Rodriguezreinoso, F. Hydrogenation of  $\alpha$ ,  $\beta$  unsaturated Aldehydes Over Polycrystalline, (111) and (100) Preferentially Oriented Pt Nanoparticles Supported on Carbon. J. Catal. 2008, 253, 159-166.
- (19) Grass, M.; Rioux, R.; Somorjai, G. Dependence of Gas-Phase Crotonaldehyde Hydrogenation Selectivity and Activity on the Size of Pt Nanoparticles (1.7-7.1 nm) Supported on SBA-15. Catal. Lett. 2009, 128, 1-8.
- (20) Prashar, A. K.; Mayadevi, S.; Nandini Devi, R. Effect of Particle Size on Selective Hydrogenation of Cinnamaldehyde by Pt Encapsulated in Mesoporous Silica. Catal. Commun. 2012, 28, 42-46.
- (21) Zhu, Y.; Zaera, F. Selectivity in the Catalytic Hydrogenation of Cinnamaldehyde Promoted by Pt/SiO2 as a Function of Metal Nanoparticle Size. Catal. Sci. Technol. 2014, 4, 955-962.

- (22) Durndell, L. J.; Parlett, C. M. A.; Hondow, N. S.; Isaacs, M. A.; Wilson, K.; Lee, A. F. Selectivity Control in Pt-Catalyzed Cinnamaldehyde Hydrogenation. Sci. Rep. 2015, 5, 9425.
- (23) Delbecq, F.; Sautet, P. Influence of Sn Additives on the Selectivity of Hydrogenation of  $\alpha$ - $\beta$ -unsaturated Aldehydes with Pt Catalysts: A Density Functional Study of Molecular Adsorption. J. Catal. 2003, 220, 115-126.
- (24) Oduro, W. O.; Cailuo, N.; Yu, K. M. K.; Yang, H.; Tsang, S. C. Geometric and Electronic Effects on Hydrogenation of Cinnamaldehyde over Unsupported Pt-Based Nanocrystals. Phys. Chem. Chem. Phys. 2011, 13, 2590-2602.
- (25) Bidaoui, M.; Especel, C.; Sabour, S.; Benatallah, L.; Saib-Bouchenafa, N.; Royer, S.; Mohammedi, O. Toward the Improvement in Unsaturated Alcohol Selectivity During  $\alpha,\beta$ -unsaturated Aldehyde Selective Hydrogenation, Using Zn as Promoter of Pt. J. Mol. Catal. A: Chem. 2015, 399, 97-105.
- (26) Siani, A.; Alexeev, O. S.; Lafaye, G.; Amiridis, M. D. The Effect of Fe on SiO<sub>2</sub>-Supported Pt Catalysts: Structure, Chemisorptive, and Catalytic Properties. J. Catal. 2009, 266, 26-38.
- (27) Zheng, R.; Porosoff, M. D.; Weiner, J. L.; Lu, S.; Zhu, Y.; Chen, J. G. Controlling Hydrogenation of CO and CC Bonds in Cinnamaldehyde Using Silica Supported Co-Pt and Cu-Pt Bimetallic Catalysts. Appl. Catal., A 2012, 419-420, 126-132.
- (28) Altmann, L.; Wang, X.; Borchert, H.; Kolny-Olesiak, J.; Zielasek, V.; Parisi, J.; Kunz, S.; Baumer, M. Influence of Sn Content on the Hydrogenation of Crotonaldehyde Catalysed by Colloidally Prepared PtSn Nanoparticles. Phys. Chem. Chem. Phys. 2015, 17, 28186-28192.
- (29) Cao, Y.; Chen, B.; Guerrero-Sánchez, J.; Lee, I.; Zhou, X.; Takeuchi, N.; Zaera, F. Controlling Selectivity in Unsaturated Aldehyde Hydrogenation Using Single-Site Alloy Catalysts. ACS Catal. 2019, 9, 9150-9157.
- (30) Cao, Y.; Guerrero-Sańchez, J.; Lee, I.; Zhou, X.; Takeuchi, N.; Zaera, F. Kinetic Study of the Hydrogenation of Unsaturated Aldehydes Promoted by CuPt<sub>x</sub>/SBA-15 Single-Atom Alloy (SAA) Catalysts. ACS Catal. 2020, 10, 3431-3443.
- (31) Luneau, M.; Lim, J. S.; Patel, D. A.; Sykes, E. C. H.; Friend, C. M.; Sautet, P. Guidelines to Achieving High Selectivity for the Hydrogenation of  $\alpha,\beta$ -Unsaturated Aldehydes with Bimetallic and Dilute Alloy Catalysts: A Review. Chem. Rev. 2020, 120, 12834-
- (32) Ball, M. R.; Proaño, L.; Nezam, I.; Lee, D.-C.; Alamgir, F.; Jones, C. W. Citral Hydrogenation over Dilute Alloy Catalysts. ChemCatChem 2023, 15, No. e202201396.
- (33) Wilson, J.; Guo, H.; Morales, R.; Podgornov, E.; Lee, I.; Zaera, F. Kinetic Measurements of Hydrocarbon Conversion Reactions on Model Metal Surfaces. Phys. Chem. Chem. Phys. 2007, 9, 3830-3852.
- (34) Tilekaratne, A.; Simonovis, J. P.; López Fagúndez, M. F.; Ebrahimi, M.; Zaera, F. Operando Studies of the Catalytic Hydrogenation of Ethylene on Pt(111) Single Crystal Surfaces. ACS Catal. 2012, 2, 2259-2268.
- (35) Simonovis, J.; Tillekaratne, A.; Zaera, F. The Role of Carbonaceous Deposits in Hydrogenation Catalysis Revisited. J. Phys. Chem. C 2017, 121, 2285-2293.
- (36) Zaera, F. Kinetics on Model Systems. In Comprehensive Inorganic Chemistry II; Reedijk, J., Poeppelmeier, K., Eds.; Elsevier: Oxford, UK, 2013, pp 39-74.
- (37) Hoffmann, F. M. Infrared Reflection-Absorption Spectroscopy of Adsorbed Molecules. Surf. Sci. Rep. 1983, 3, 107-192.
- (38) Zaera, F. New Advances in the Use of Infrared Absorption Spectroscopy for the Characterization of Heterogeneous Catalytic Reactions. Chem. Soc. Rev. 2014, 43, 7624-7663.
- (39) Zaera, F. In-Situ and Operando Spectroscopies for the Characterization of Catalysts and of Mechanisms of Catalytic Reactions. J. Catal. 2021, 404, 900-910.
- (40) Beccat, P.; Bertolini, J. C.; Gauthier, Y.; Massardier, J.; Ruiz, P. Crotonaldehyde and Methylcrotonaldehyde Hydrogenation over Pt(111) and Pt<sub>80</sub>fe<sub>20</sub>(111) Single Crystals. J. Catal. 1990, 126, 451-456.

- (41) Zaera, F.; Somorjai, G. A. Hydrogenation of Ethylene over Platinum (111) Single-Crystal Surfaces. *J. Am. Chem. Soc.* **1984**, *106*, 2288–2293.
- (42) Tillekaratne, A.; Simonovis, J. P.; Zaera, F. Ethylene Hydrogenation Catalysis on Pt(111) Single-Crystal Surfaces Studied by Using Mass Spectrometry and in Situ Infrared Absorption Spectroscopy. *Surf. Sci.* **2016**, *652*, 134–141.
- (43) Zaera, F. The Surface Chemistry of Metal-Based Hydrogenation Catalysis. ACS Catal. 2017, 7, 4947–4967.
- (44) Somorjai, G. A.; Zaera, F. Heterogeneous Catalysis on the Molecular Scale. *J. Phys. Chem.* **1982**, *86*, 3070–3078.
- (45) Dostert, K.-H.; O'Brien, C. P.; Mirabella, F.; Ivars-Barceló, F.; Attia, S.; Spadafora, E.; Schauermann, S.; Freund, H.-J. Selective Partial Hydrogenation of Acrolein on Pd: A Mechanistic Study. *ACS Catal.* **2017**, *7*, 5523–5533.
- (46) Sá, J.; Medlin, J. W. On-the-Fly Catalyst Modification: Strategy to Improve Catalytic Processes Selectivity and Understanding. *ChemCatChem* **2019**, *11*, 3355–3365.
- (47) Kiskinova, M.; Szabó, A.; Yates, J. T. CO adsorption on Pt(111) modified with sulfur. *J. Chem. Phys.* **1988**, 89, 7599–7608.
- (48) Rupprechter, G.; Dellwig, T.; Unterhalt, H.; Freund, H. J. CO Adsorption on Ni(100) and Pt(111) Studied by Infrared, Visible Sum Frequency Generation Spectroscopy: Design and Application of an SFG-Compatible UHV-High-Pressure Reaction Cell. *Top. Catal.* **2001**, *15*, 19–26.
- (49) Hopster, H.; Ibach, H. Adsorption of CO on Pt(111) and Pt 6(111) × (111) Studied by High Resolution Electron Energy Loss Spectroscopy and Thermal Desorption Spectroscopy. *Surf. Sci.* **1978**, 77, 109–117.
- (50) Hayden, B. E.; Kretzschmar, K.; Bradshaw, A. M.; Greenler, R. G. An Infrared Study of the Adsorption of CO on a Stepped Platinum Surface. *Surf. Sci.* **1985**, *149*, 394–406.
- (51) Zaera, F.; Liu, J.; Xu, M. Isothermal Study of the Kinetics of Carbon Monoxide Oxidation on Pt(111): Rate Dependence on Surface Coverages. *J. Chem. Phys.* **1997**, *106*, 4204–4215.
- (52) Zaera, F.; Godbey, D.; Somorjai, G. A. Methylcyclopentane Conversion over Platinum Single Crystal Surfaces: Evidence for the Cyclic Mechanism of *n*-Hexane Isomerization. *J. Catal.* **1986**, *101*, 73–80.
- (53) Ainsworth, M. K.; McCoustra, M. R. S.; Chesters, M. A.; Sheppard, N.; De La Cruz, C. An Infrared Study of Ethene and CO Coadsorption on Pt[111] and a Pt/SiO<sub>2</sub> Catalyst: Ambiguities in the Interpretation of Difference Spectra. *Surf. Sci.* **1999**, *437*, 9–17.
- (54) Simonovis, J.; Zaera, F. Abrupt Increase in Hydrogen Diffusion on Transition-Metal Surfaces During Hydrogenation Catalysis. *Chem. Sci.* **2016**, *7*, 4660–4666.
- (55) Vannice, M. A.; Sen, B. Metal-Support Effects on the Intramolecular Selectivity of Crotonaldehyde Hydrogenation over Platinum. *J. Catal.* **1989**, *115*, 65–78.
- (56) Meng, Y.; Xia, S.; Zhou, X.; Pan, G. Mechanism of Selective Hydrogenation of Cinnamaldehyde on Ni-Pt(111) with Different Structures: A Comparative Study. *Chem. Phys. Lett.* **2020**, 740, 137049.
- (57) Greenler, R. G. Infrared Study of Adsorbed Molecules on Metal Surfaces by Reflection Techniques. *J. Chem. Phys.* **1966**, 44, 310–315.
- (58) de Jesús, J. C.; Zaera, F. Double-Bond Activation in Unsaturated Aldehydes: Conversion of Acrolein to Propene and Ketene on Pt(111) Surfaces. J. Mol. Catal. A: Chem. 1999, 138, 237–240
- (59) de Jesús, J. C.; Zaera, F. Adsorption and Thermal Chemistry of Acrolein and Crotonaldehyde on Pt(111) Surfaces. *Surf. Sci.* **1999**, 430, 99–115.
- (60) Skinner, P.; Howard, M. W.; Oxton, I. A.; Kettle, S. F. A.; Powell, D. B.; Sheppard, N. Vibrational Spectra and the Force Field of Ethylidyne Tricobalt Nonacarbonyl: Analogies with Spectra from the Chemisorption of Ethylene Upon the Pt (111) Crystal Face. *J. Chem. Soc., Faraday Trans.* 2 **1981**, 77, 1203–1215.

- (61) Sheppard, N. Surface Studies by IR Spectroscopy. In *Encyclopedia of Spectroscopy and Spectrometry* 2nd ed.; John, L., Ed.; Academic Press: Oxford, 2010; pp 2813–2821.
- (62) Beebe, T. P., Jr; Albert, M. R.; Yates, J. T., Jr Infrared Spectroscopic Observation and Characterization of Surface Ethylidyne on Supported Palladium on Alumina. J. Catal. 1985, 96, 1–11.
- (63) Lapinski, M. P.; Ekerdt, J. G. In Situ Fourier Transform Infrared Study of Ethylene Surface Reaction Kinetics on Alumina-Supported Nickel. *J. Phys. Chem.* **1992**, *96*, 5069–5077.
- (64) Weisel, M. D.; Hoffmann, F. M.; Mims, C. A. In-Situ Ft-Iras at Elevated Pressure: Stability and Decomposition Kinetics of Reaction Intermediates. *J. Electron Spectrosc. Relat. Phenom.* **1993**, 64–65, 435–439
- (65) Cremer, P. S.; Su, X.; Shen, Y. R.; Somorjai, G. A. Ethylene Hydrogenation on Pt(111) Monitored in Situ at High Pressures Using Sum Frequency Generation. *J. Am. Chem. Soc.* **1996**, *118*, 2942–2949.
- (66) Kaltchev, M.; Thompson, A. W.; Tysoe, W. T. Reflection-Absorption Infrared Spectroscopy of Ethylene on Palladium(111) at High Pressure. *Surf. Sci.* **1997**, *391*, 145–149.
- (67) Ohtani, T.; Kubota, J.; Kondo, J. N.; Hirose, C.; Domen, K. In-Situ Observation of Hydrogenation of Ethylene on a Pt(111) Surface under Atmospheric Pressure by Infrared Reflection Absorption Spectroscopy. *J. Phys. Chem. B* **1999**, 103, 4562–4565.
- (68) Wasylenko, W.; Frei, H. Direct Observation of Surface Ethyl to Ethane Interconversion Upon  $C_2H_4$  Hydrogenation over  $Pt/Al_2O_3$  Catalyst by Time-Resolved FT-IR Spectroscopy. *J. Phys. Chem. B* **2005**, *109*, 16873–16878.
- (69) Kweskin, S. J.; Rioux, R. M.; Song, H.; Komvopoulos, K.; Yang, P.; Somorjai, G. A. High-Pressure Adsorption of Ethylene on Cubic Pt Nanoparticles and Pt(100) Single Crystals Probed by in Situ Sum Frequency Generation Vibrational Spectroscopy. *ACS Catal.* **2012**, *2*, 2377–2386.
- (70) Krooswyk, J. D.; Waluyo, I.; Trenary, M. Simultaneous Monitoring of Surface and Gas Phase Species During Hydrogenation of Acetylene over Pt(111) by Polarization-Dependent Infrared Spectroscopy. *ACS Catal.* **2015**, *5*, 4725–4733.
- (71) Heyden, B.; Bradshaw, A. M. The Adsorption of CO on Pt(111) Studied by Infrared Reflection—Absortion Spectroscopy. *Surf. Sci.* **1983**, 125, 787–802.
- (72) Malik, I. J.; Trenary, M. Infrared Reflection-Absorption Study of the Adsorbate-Substrate Stretch of CO on Pt(111). *Surf. Sci.* 1989, 214, L237–L245.
- (73) Gland, J. L.; Fischer, D. A.; Shen, S.; Zaera, F. Displacement of Carbon Monoxide Chemisorbed on Metals by Hydrogen. *J. Am. Chem. Soc.* **1990**, *112*, 5695–5697.
- (74) Horiuti, J.; Miyahara, K. Hydrogenation of Ethylene on Metallic Catalysts," NSRDS-NBC No. 13; National Bureau of Standards, 1968.
- (75) Tsung, C.-K.; Kuhn, J. N.; Huang, W.; Aliaga, C.; Hung, L.-I.; Somorjai, G. A.; Yang, P. Sub-10 nm Platinum Nanocrystals with Size and Shape Control: Catalytic Study for Ethylene and Pyrrole Hydrogenation. *J. Am. Chem. Soc.* **2009**, *131*, 5816–5822.
- (76) Cremer, P. S.; Su, X.; Shen, Y. R.; Somorjai, G. The Hydrogenation and Dehydrogenation of Isobutene on Pt(111) Monitored by IR-Visible Sum Frequency Generation and Gas Chromotography. *J. Chem. Soc., Faraday Trans.* 1996, 92, 4717–4722.
- (77) Davis, S. M.; Zaera, F.; Somorjai, G. A. The Reactivity and Composition of Strongly Adsorbed Carbonaceous Deposits on Platinum. Model of the Working Hydrocarbon Conversion Catalyst. *J. Catal.* **1982**, 77, 439–459.
- (78) Jung, U.; Elsen, A.; Li, Y.; Smith, J. G.; Small, M. W.; Stach, E. A.; Frenkel, A. I.; Nuzzo, R. G. Comparative in Operando Studies in Heterogeneous Catalysis: Atomic and Electronic Structural Features in the Hydrogenation of Ethylene over Supported Pd and Pt Catalysts. ACS Catal. 2015, 5, 1539–1551.
- (79) Zaera, F. On the Mechanism for the Hydrogenation of Olefins on Transition-Metal Surfaces: The Chemistry of Ethylene on Pt(111). *Langmuir* **1996**, *12*, 88–94.

- (80) Zaera, F. Key Unanswered Questions About the Mechanism of Olefin Hydrogenation Catalysis by Transition-Metal Surfaces: A Surface-Science Perspective. *Phys. Chem. Chem. Phys.* **2013**, *15*, 11988–12003.
- (81) Krooswyk, J. D.; Kruppe, C. M.; Trenary, M. In-Situ Spectroscopic Monitoring of the Ambient Pressure Hydrogenation of C<sub>2</sub> to Ethane on Pt(111). *Surf. Sci.* **2016**, 652, 142–147.
- (82) Delbecq, F.; Sautet, P. A Density Functional Study of Adsorption Structures of Unsaturated Aldehydes on Pt(111): A Key Factor for Hydrogenation Selectivity. *J. Catal.* **2002**, 211, 398–406.
- (83) Loffreda, D.; Jugnet, Y.; Delbecq, F.; Bertolini, J. C.; Sautet, P. Coverage Dependent Adsorption of Acrolein on Pt(111) from a Combination of First Principle Theory and Hreels Study. *J. Phys. Chem. B* **2004**, *108*, 9085–9093.
- (84) Loffreda, D.; Delbecq, F.; Vigne, F.; Sautet, P. Catalytic Hydrogenation of Unsaturated Aldehydes on Pt(111): Understanding the Selectivity from First-Principles Calculations. *Angew. Chem., Int. Ed.* **2005**, *44*, 5279–5282.
- (85) Murillo, L. E.; Menning, C. A.; Chen, J. G. Trend in the CC and CO Bond Hydrogenation of Acrolein on Pt-M (M = Ni, Co, Cu) Bimetallic Surfaces. *J. Catal.* **2009**, 268, 335–342.
- (86) Nayakasinghe, M. T.; Guerrero-Sánchez, J.; Takeuchi, N.; Zaera, F. Adsorption of Crotonaldehyde on Metal Surfaces: Cu Vs Pt. *J. Chem. Phys.* **2021**, *154*, 104701.
- (87) Ruvalcaba, R.; Guerrero-Sanchez, J.; Takeuchi, N.; Zaera, F. Crotonaldehyde Adsorption on Cu-Pt Surface Alloys: A Quantum Mechanics Study. *Chemistry* **2023**, *5*, 463–478.
- (88) Dong, Y.; Zaera, F. Selectivity in Hydrogenation Catalysis with Unsaturated Aldehydes: Parallel Versus Sequential Steps. *J. Phys. Chem. Lett.* **2018**, *9*, 1301–1306.
- (89) Dong, Y.; Zaera, F. Kinetics of Hydrogen Adsorption During Catalytic Reactions on Transition Metal Surfaces. *Catal. Sci. Technol.* **2017**, *7*, 5354–5364.
- (90) Sinfelt, J. H. Catalysis by Alloys and Bimetallic Clusters. *Acc. Chem. Res.* **1977**, *10*, 15–20.
- (91) Ponec, V. Exchange and Reforming Reactions of Hydrocarbons on Metals and Alloys. In *The Chemical Physics of Solid Surfaces and Heterogeneous Catalysis*; King, D. A., Woodfuff, D. P., Eds.; Elsevier: Amsterdam, 1982; Vol. 4, pp 365–395.
- (92) Rong, H.; Niu, Z.; Zhao, Y.; Cheng, H.; Li, Z.; Ma, L.; Li, J.; Wei, S.; Li, Y. Structure Evolution and Associated Catalytic Properties of Pt-Sn Bimetallic Nanoparticles. *Chem.—Eur. J.* **2015**, *21*, 12034–12041.
- (93) Shi, J.; Zhang, M.; Du, W.; Ning, W.; Hou, Z. SnO<sub>2</sub>-Isolated Pt<sub>3</sub>Sn Alloy on Reduced Graphene Oxide: An Efficient Catalyst for Selective Hydrogenation of C = O in Unsaturated Aldehydes. *Catal. Sci. Technol.* **2015**, *5*, 3108–3112.
- (94) Stassi, J.; Méndez, J.; Vilella, I.; de Miguel, S.; Zgolicz, P. Synthesis of PtSn Nanoparticles on Carbon Materials by Different Preparation Methods for Selective Catalytic Hydrogenation of Citral. *Chem. Eng. Commun.* **2020**, 207, 1074–1091.
- (95) Kahsar, K. R.; Johnson, S.; Schwartz, D. K.; Medlin, J. W. Hydrogenation of Cinnamaldehyde over Pd/Al2O3 Catalysts Modified with Thiol Monolayers. *Top. Catal.* **2014**, *57*, 1505–1511.
- (96) Zaera, F. Designing Sites in Heterogeneous Catalysis: Are We Reaching Selectivities Competitive with Those of Homogeneous Catalysts? *Chem. Rev.* **2022**, *122*, 8594–8757.